Since January 2020 Elsevier has created a COVID-19 resource centre with free information in English and Mandarin on the novel coronavirus COVID-19. The COVID-19 resource centre is hosted on Elsevier Connect, the company's public news and information website.

Sensors & Actuators: B. Chemical 325 (2020) 128780

Contents lists available at ScienceDirect

Sensors and Actuators: B. Chemical

journal homepage: www.elsevier.com/locate/snb

Rapid Enrichment and Ultrasensitive Detection of Influenza A Virus in Human Specimen using Magnetic Quantum Dot Nanobeads Based Test Strips

Zikun Bai [a,b,1], Hongjuan Wei [a,b,1], Xingsheng Yang [a,c], Yanhui Zhu [a,b], Yongjin Peng [a,b], Jing Yang [a,b], Chongwen Wang [a,c,*], Zhen Rong [a,b,*], Shengqi Wang [a,b,*]

[a] Beijing Institute of Radiation Medicine, Beijing 100850, PR China
[b] Beijing Key Laboratory of New Molecular Diagnosis Technologies for Infectious Diseases, Beijing 100850, PR China
[c] College of Life Sciences, Anhui Agricultural University, Hefei 230036, PR China

ARTICLE INFO

Keywords:
Magnetic quantum dot nanobead
Magnetic enrichment
Lateral flow assay
Influenza A virus
Nasopharyngeal swab

ABSTRACT

Influenza A virus (IAV) possesses a high infectivity and pathogenicity, and can lead to severe respiratory infection with similar symptoms caused by some other common respiratory viruses. Lateral flow assay (LFA) has been widely deployed in remote settings as a rapid and reliable approach for point-of-care detection of infectious pathogens. However, it still remains challenging to detect IAV virions using LFA from clinical samples such as nasopharyngeal or throat swabs, because their various components and high viscosity can decrease flow velocity and lead to the nonspecific adsorption of nanoparticle labels on the sensing membrane. Herein, we demonstrated a magnetic quantum dot nanobeads (MQBs) based LFA for magnetic enrichment and fluorescent detection of IAV virions in clinical specimens. In this study, MQBs were synthesized and then conjugated with IAV-specific antibody to efficiently enrich IAV virions from complex biological matrix, but also serve as highly bright fluorescent probes in lateral flow strips. This assay can achieve quantitative detection of IAV virions with a low limit of detection down to 22 pfu mL^{-1} within 35 minutes, and show good specificity between influenza B virus and two adenovirus strains. Furthermore, the presented platform was able to directly detect IAV virions spiked in nasopharyngeal swab dilution, indicating its stability and feasibility in clinical applications. Thus, this point-of-care detection platform holds great promise as a broadly applicable approach for the rapid diagnosis of influenza A.

1. Introduction

Influenza is the most significant cause of human respiratory infection, and posses a serious threat to human health [1]. Influenza A, instead of influenza B and parainfluenza, is likely to cause severe worldwide pandemics. Since 1700, there have been several serious outbreaks of influenza A, taking the life-threatening problem to people around the world. Especially in 1918, the pandemic vulnerated about 50 million all-aged people death [2]. Recently, the influenza A H1N1 2009 virus strain (A/2009/H1N1), a drift from human H1N1 subtype to a swine H1N1 subtype, caused a raging pandemic among all mankind which took more than 18000 death [3]. The U.S. CDC estimates that influenza has induced 9.2 million to 35.6 million illnesses, including 12,000 to 56,000 deaths annually in the U.S. alone over the six seasons from 2010–2011 through 2015–2016 [4].

Rapid and accurate diagnosis of influenza is critical for timely medical intervention and appropriate prescription such as oseltamivir to improve therapeutic effect and prevent possible epidemics breakout. It can also reduce the observation time of suspected patients and avoid abuse of antibiotics [5]. The recommended time to take antiviral treatment is within two days from illness onset [6]. However, the current "gold standard" diagnostic method in hospital, namely virus culture, unfortunately requires several days [7,8]. Moreover, influenza shares similar clinical symptoms caused by other respiratory tract infections, which sets obstacles for accurate diagnosis [9]. Influenza A virus (IAV) has two surface glycoproteins including hemagglutinin (HA)

* Corresponding authors.
E-mail addresses: wangchongwen1987@126.com (C. Wang), rongzhen0525@sina.com (Z. Rong), sqwang@bmi.ac.cn (S. Wang).
[1] Z.-K.B. and H.-J.W. contributed equally to this work.

https://doi.org/10.1016/j.snb.2020.128780
Received 17 February 2020; Received in revised form 17 August 2020; Accepted 17 August 2020
Available online 21 August 2020

and neuraminidase (NA), by which the IAVs can be subtyped. There are 18 different HA subtypes and 11 different NA subtypes by far. A test assay that is able to differentiate between influenza A and other common respiratory infections can facilitate the implement of timely and rational treatment options, which are conducive to the sanitation safety of individuals and the public. Thus, development of diagnostic platform with short assay time and superior accuracy is still essential for prevent of possible epidemics breakout.

In recent decades, point-of-care testing (POCT) has attracted much attention because of its easy workflow, short assay time, and low cost. Application of POCT in the diagnosis of patients with symptoms of respiratory tract infection can effectively reduce diagnostic time, treatment cycle and the corresponding treatment costs [10]. A variety of immunosensors, such as lateral flow assays (LFAs) [11,12], and microfluidic devices [7,13–16], have been used in the rapid diagnosis of influenza A and shown their advantages of convenience and rapidity. These strategies can raise the diagnosis chronergy, but the high false-negative results are not conducive to the individual treatment (e.g., the delayed antiviral drugs, or overuse of antibiotics) and the safety of public health (e.g., inadequate pandemic control, or virus resistance) [9,17]. Sensitivity and accuracy of POCT are the key issues that should be dramatically taken concern on.

Nasopharyngeal swabs, throat swabs, nasopharyngeal wash and saliva, which all have a high virus titer, can be used as the effective specimen formats collected from clinically suspected cases [18,19]. However, these collected specimens with a complex internal matrix would interfere with test results due to their various components and high viscosity that can decrease flow velocity and lead to the nonspecific adsorption of nanoparticle labels on the sensing substrates. To overcome this drawback, these specimens should be diluted by wash buffer and only a small aliquot of processed sample would be used for subsequent testing [20,21]. This pretreatment can directly worsen the analytical performance because of the loss of target analytes.

Immunomagnetic nanobeads can recognize and enrich target analytes in complex matrix with an external magnetic field [15]. Recently, magnetic quantum dot nanobeads (MQBs) have been prepared and deployed in LFA to enable immune enrichment, fluorescent labeling, and rapid detection of cancer markers, toxins, and bacteria [22–25]. These approaches extremely extend the application of LFA in the analysis of targets in real samples such as clinical serum and food samples. However, it remains challenging to detect trace amount of disease biomarker targets, such as antigens and viruses, in human respiratory tract specimens due to the low viral load and high viscosity. Given the current outbreak of the 2019 coronavirus disease, it's urgent to establish novel analysis techniques for the enrichment and detection of respiratory viruses in human specimens. Herein, we present the MQBs-based fluorescent LFA for rapid enrichment and ultrasensitive detection of IAV virions in human specimen. Superparamagnetic $MnFe_2O_4$ nanobead cores were synthesized via a solvothermal method and coated with positively-charged polyethyleneimine (PEI) layer to electrostatically adsorb hundreds of quantum dots (QDs). The as-synthesized MQBs with strong magnetic property and bright fluorescence were further conjugated with IAV-specific antibody to enrich IAV virions in nasopharyngeal swab dilution, and act as the fluorescent labels in lateral flow strips. This magnetic immunoseparation and enrichment process can serve as a simple and reliable pretreatment method to improve the quality of clinical samples for POCT applications. Additionally, the fluorescence signal can be captured by the smartphone-based device and processed through the in-house algorithm to achieve quantitative analysis. The signal acquisition, analysis and processing device can further improve the sensitivity and anti-interference ability of the MQBs-based LFA. The detection system, including virus enrichment, lateral flow detection, and signal processing, can achieve a low limit of detection down to 22 pfu mL^{-1} IAV virions within 35 minutes, and show good specificity between influenza B virus and two adenovirus strains. This simple and ultrasensitive approach can enable emergent and accurate diagnosis of influenza A from various patients with respiratory tract infection, and facilitate the medical treatment of individual and the control of epidemic.

2. Experimental section

2.1. Materials

N-(3-(dimethylamino) propyl)-N′-ethylcarbodiimide hydrochloride (EDC), N-hydroxysuccinimide (NHS), Polyetherimide (PEI), bovine serum albumin (BSA), fetal calf serum (FBS), 2-(N-morpholino) ethanesulfonic (MES) monohydrate were purchased from Sigma-Aldrich (USA). Carboxyl-functionalized CdSe/ZnS QDs (CdSe-MPA-625) were provided by Mesolight Technology (Suzhou, China). Nitrocellulose (NC) membranes were obtained from Sartorius (CN140 and CN95, Spain) and Millipore (HFC135 and HFC90, USA). Goat anti-mouse IgG antibody was purchased from Sangon Biotech Co., Ltd. (Shanghai, China). IAV and HAdV monoclonal antibodies were purchased from Xinxin Bio, Ltd. (Jiangsu, China). Two IAV strains (H1N1 FM1/A, and H1N1 2009/A), influenza B virus (IBV) and two human adenovirus strains (HAdV5 and HAdV55) were cultured in chick embryos in our lab.

2.2. Preparation and antibody conjugation of MQBs

First, the 200-nm-diameter superparamagnetic $MnFe_2O_4$ magnetic nanobeads (MBs) were synthesized by using a solvothermal method [26]. Subsequently, the as-prepared MBs were deposited with a thin layer of electropositive PEI, followed by mixing with CdSe/ZnS QDs (625 nm) to form MQBs. The obtained MQBs will be washed with water three times before resuspension in ethanol for long-term storage. The fluorescent intensity can remain stable for 3 months in ethanol.

Then, 1 mL of MQBs (~1 mg/mL) underwent buffer exchange into 0.5 mL of MES (0.1 M, PH 6.0) using a rubidium magnet, and were activated by NHS/EDC coupling reagents (1 mM/0.5 mM) for 15 min. After that, the particles were separated by magnet and then incubated with 10 μg of IAV capture antibody for 2 h under gentle shaking at 800 rpm in 0.2 mL of 10 mM PBS, 0.05% Tween-20. Excessed binding sites were blocked by 20 μL of 10 wt% BSA for 30 min. The resultant antibody-conjugated MQBs were magnetically washed twice with PBST and stored in 0.2 mL of PBST with 1 wt% BSA stock buffer. The obtained conjugates could be lyophilized and stored for at least 2 months without obvious impact on analytical performance, which indicates the long-term stable affinity of lyophilized antibody.

2.3. Preparation of test strips

IAV detection antibody (0.6 mg mL^{-1}) and polyclonal goat anti-mouse IgG (0.7 mg mL^{-1}) were sprayed on NC membranes as test and control lines at a jetting rate of 1 μL cm^{-1} by using Biodot XYZ3050 plotter. The NC membranes were then dried at 37 °C for 1.5 h. Then, NC membranes, sample pad and absorbent membranes were assembled on a plastic backing plate, and split into 3 mm-width strips for further use.

2.4. Detection of influenza A virus

IAV virions were cultured in chick embryo and evaluated by using plaque assays as shown in **Fig. S1**. Then, quantified IAV virions were diluted in buffer solution (10 mM PBS, pH 7.4, 0.05% tween-20) to prepare standard solutions ranging from 10 to 1×10^6 pfu mL^{-1}. Then, 500 μL of prepared IAV virion dilutions were incubated with 2 μL of antibody-conjugated MQBs (~5 mg/mL) in a tube for 25 min under gentle shaking. After incubation, the immune complexes were separated and enriched with a rubidium magnet and then suspended in sample solution (65 μL PBS, 2% Tween-20, 2% FBS, 1% BSA), which were further added to the sample pads of lateral flow strips to allow for an incubation of 10 min. To simulate clinical specimens, nasopharyngeal

swabs collected from healthy people were soaked in 0.5 mL of buffer solution and then spiked with IAV virions ranging from 100 to 2000 pfu mL^{-1}. The samples were tested by the MQBs-based LFA following the above described procedure. The resultant strips were read out by our in-house developed smartphone-based fluorescent lateral flow strip reader.

2.5. Analysis of fluorescence signal

A smartphone-based fluorescence measurement and analysis device was developed based on our previous work (**Fig. S2**) [22]. Two symmetrical ultraviolet LEDs (365 nm, 1 W) were filtered by a 365 nm bandpass filter and used to excite the captured MQBs on the test and control lines of the test strip in a dark cavity. The 625 nm fluorescence emission passed through a bandpass filter to remove background noise, and was collected by the smartphone CMOS image sensor after being focused by an external optical lens. An in-house designed Android APP was used to process images and analyze data. As shown in **Fig. S3**, some basic sample information can be logged in the APP, and then be recorded with the analysis result in a txt file, which can be transmitted to other terminals through Bluetooth or Wireless LAN.

3. Results and discussion

3.1. Assay principle

We developed an LFA-based detection and analysis system that can efficiently enrich and ultrasensitively detect IAV virions. As shown in Fig. 1, the sample on the swab was dissolved into 0.5 mL diluent, and then IAV antibody-conjugated MQBs were dispersed in the diluent to fully mix with various components in the dissolved sample. During the incubation process, the MQBs probes in solution would specifically recognize and capture free virions hidden in the secretion. A rubidium magnet with strong permanent magnetic property was applied to enrich the MQB-IAVs conjugates formed in solution and to remove the impurities in the sample (e.g. blood, food debris, et al.) that may interfere with the analysis result. Meanwhile, the magnetic enrichment method could capture virions in the entire sample diluent. As a comparison, current commercial LFA detection kits can utilize only 10 to 25 percent of the sample diluent. As such, target IAV virions in this assay were enriched by 4 to 10 times that of commercial method. Then, the magnetically-separated immune complexes were suspended in loading buffer and dropped onto the sample pad to allow for the capillary-driven immigration towards the NC membrane. IAV-captured MQBs were coupled with IAV detection antibody sprayed on the test line and the excessed MQBs were bound by goat anti-mouse IgG sprayed on the control line. After the capillarity, the bright 625 nm fluorescence signals were emitted from the MQBs immobilized on test and control lines under the excitation of 365 nm ultraviolet light. The fluorescence signals would be imaged by using the smartphone-based detection device. Subsequently, fluorescence intensity (FI) value was read out and background signal baseline was recognized and removed. The processed FI value was regressively fitted to determine concentration by the in-house algorithm. Overall, IAV virions in complex biological samples can be directly enriched and captured in this assay. This platform possesses several distinct features as follows: (i) simple and rapid detection operation principle based on lateral flow strip; (ii) high applicability in complex biological matrixes without obvious interference after magnetic separation and buffer exchange; and (iii) improved sensitivity due to magnetic enrichment ability and high luminescent signal of MQBs.

3.2. Characterization of MQBs

In this study, the $MnFe_2O_4$@PEI@QDs MQBs, which had strong magnetic response capability and highly bright fluorescent signal on each particle, were assembled to be applied in LFA for magnetic enrichment and fluorescent detection of IAV virions. The 200-nm-diameter $MnFe_2O_4$ cores were synthesized by a modified solvothermal reaction [27], by which the magnetic cores had a superior performance based on homogenization control. The positively-charged PEI was wrapped on the surface of the magnetic core as an “adhesive”, and the surface electrical property was converted to positively charged status, which provided suitable conditions for electrostatic adsorption of negatively-charged QDs. As shown in **Fig. S4A-C**, the zeta potentials of $MnFe_2O_4$, $MnFe_2O_4$@PEI, and $MnFe_2O_4$@PEI@QDs were −37.1, 43.6, and −37.1 mV, respectively, which confirms the successful preparation of MQBs. As shown in Fig. 2A, the QDs are almost fully absorbed on the surface of magnetic cores with free of gaps. It can be estimated that approximately 645 QDs can be absorbed on the surface of each magnetic core. The calculation equation was represented by $n = (4\pi(R+r)^2)/\pi r^2$, where n, R and r represented the QDs quantity, the radius of magnetic core and the radius of QD, respectively. The fluorescence intensity of MQBs was estimated approximately 114 times stronger than that of QDs

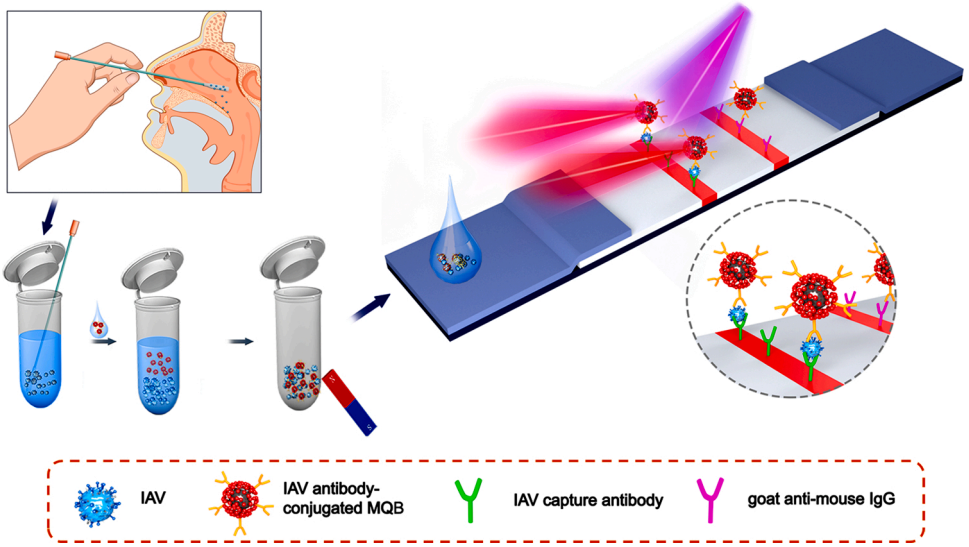

Fig. 1. Schematic illustration of IAV virion detection using MQBs-based LFA. Nasopharyngeal swab specimen was collected, diluted, and mixed with antibody-conjugated MQBs. After incubation, immunocomplexes were magnetically enriched and loaded onto the sample pad for lateral flow, forming sandwich complexes on T line.

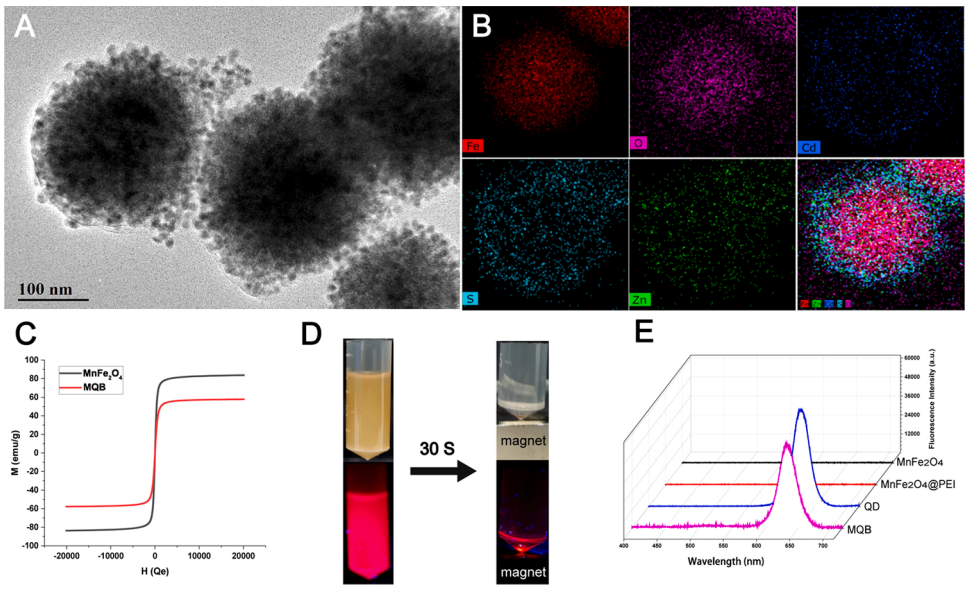

Fig. 2. Characterization of MQBs. (A) TEM image. (B) Elemental mapping images. (C) Magnetic hysteresis curves. (D) Magnetic separation performance in the solution. (E) Fluorescence spectra of nanomaterials under ultraviolet light.

at the same nanoparticle concentration (**Fig. S5**). The element mapping was taken to further characterize the adsorption of QDs on the magnetic core. As shown in Fig. 2B, a strong intensity of iron and oxygen elements can be measured in the central area, and the cadmium element contained in QD is dense in the periphery, which can indicate the efficient adsorption of QDs. The magnetic response ability is directly associated with the sample enrichment efficiency, which would be reduced after the assembly of the $MnFe_2O_4$@PEI@QDs nanobeads. The hysteresis curves of these magnetic particles were measured (Fig. 2C) and showed that the saturation magnetization decreased from 83.7 to 57.7 emu/g after the assembly, which was still much higher than some other reported magnetic nanospheres with virus-capturing function [28,29]. The synthesized MQBs can complete magnetic aggregation in 30 seconds in the magnetic field provided by a rubidium magnet (Fig. 2D). To

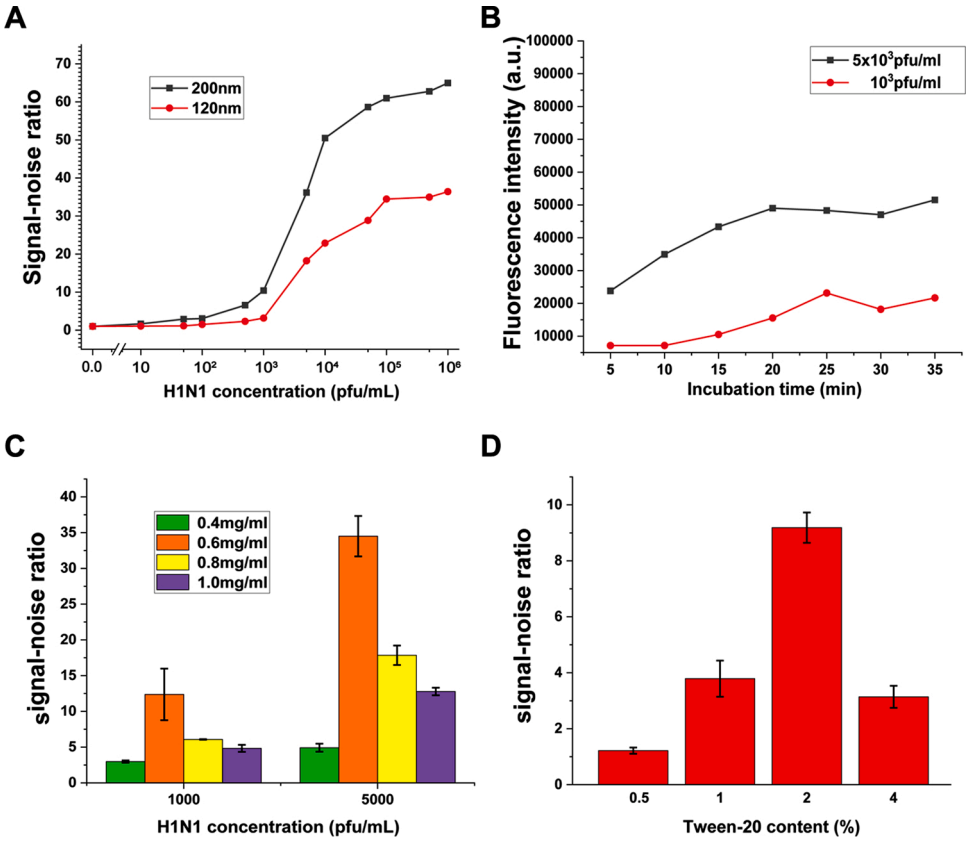

Fig. 3. Optimization of assay parameters. Effects of (A) $MnFe_2O_4$ core diameters, (B) incubation time, (C) detection antibody concentration, and (D) Tween-20 concentration. Error bars represent the standard deviation of three repetitive experiments.

determine the fluorescence property of MQBs, the emission spectra were measured by using a spectrometer (USB2000+, Ocean Optics). As shown in Fig. 2E, both the QDs and $MnFe_2O_4$@PEI@QDs emitted red fluorescence at 625 nm under the excitation of ultraviolet light, indicating that $MnFe_2O_4$@PEI did not affect the emission light. Moreover, the antibody-conjugated MQBs can remain stable at least 30 days in stock buffer and sample solution (**Fig. S6A-B**).

3.3. Optimization of MQBs-based LFA

Given the IAV virion diameter of about 80 to 100 nm, the magnetic responsiveness of $MnFe_2O_4$ cores should be strong enough to capture and enrich the IAV virions. Furthermore, the magnetic responsiveness is positively correlated with the size, but the larger particles are, the stronger steric hindrance is when the immune complexes immigrate through the NC membrane. Accordingly, MQBs with two different MB core sizes of 120 and 200 nm were tested and compared in this assay. On the basis of signal-noise ratio (SNR), analytical performances of this assay were evaluated to determine the optimal assay parameters to improve the sensitivity of specific immune binding and inhibit nonspecific adsorption. Fig. 3**A** showed SNR curves for detection of IAV virions ranged from 10 to 1×10^6 pfu mL^{-1} using two different sized MQBs. The SNR was calculated by $F/F_0 \times 100\%$, where F and F_0 are FI values of test lines for IAV virion-spiked and IAV virion-free solutions, respectively. The results indicated that the SNRs of both groups increased with increasing virus concentration, but the 200-nm-diameter MB cores resulted in significantly improved SNRs, which can be attributed to the stronger immune binding and IAV virion capturing ability of larger MBs. As a result, MQBs with 200-nm-diameter $MnFe_2O_4$ cores were applied in this assay.

According to the immunoreaction kinetics analysis, the performance of MQBs on virion capture is closely related to the incubation time, but there existed a contradiction between signal intensity and rapidity to compromise. Two different concentrations of IAV virions (1×10^3 and 5×10^3 pfu mL^{-1}) were analyzed to set optimal incubation time. These two sets of IAV virions (1×10^3 and 5×10^3 pfu mL^{-1}) were incubated with the same amount of MQBs from 5 min to 35 min with an interval time of 5 min. Then, the magnetically-separated immunocomplexes were further added to the sample pads of lateral flow strips to allow for an assay time of 10 min before signal capture and analysis. The results in Fig. 3**B** showed that the FI gradually increased with the extension of incubation time and reached saturation after 25 min for these two concentrations of IAV virions. Thus, an incubation time of 25 min was utilized in this assay. It should be noted that the resulting MQB-IAVs immunocomplexes can be re-suspended in sample solution without obvious aggregation as shown in **Fig. S7A**. The immunocomplexes can also exhibit stable fluorescence signals in sample solution for 7 days (**Fig. S7B**), indicating a good long-term stability.

The pore size of NC membrane affects the capillary velocity, thus tuning the immigration of MQBs and the immune affinity on the T/C lines. Four different NC membranes (CN140, HFC135, CN95, HFC90) were tested through the comparison of SNR at two IAV virion concentrations. The time consumed by aqueous solution to immigrate a 4-cm-long membrane is 110–165 s, 120–150 s, 90–135 s, and 81–99 s, respectively, which can reflect the pore size of NC membrane. As shown in **Fig. S8**, the SNRs for two large-pore-size NC membranes (CN95, HFC90) are significantly higher than that for two small-pore-size NC membranes (CN140, HFC135). This can be attributed to a stronger background signal due to MQBs probes blocked by the relatively small NC membrane pore. Furthermore, CN95 membrane resulted in the highest SNR, thus it was utilized in this assay.

In order to further improve the assay performance, the concentration of detection antibody underwent meticulous optimization. Four adjacent gradient concentrations of the detection antibody (0.4, 0.6, 0.8, 1.0 mg mL^{-1}) were used to detect two concentrations of IAV virions. Fig. 3**C** showed that 0.6 mg mL^{-1} of detection antibody induced the best SNR, indicating it was the optimal concentration of detection antibody in this assay.

The loading buffer also affects the analytical performance of the LFA through tuning the steric hindrance in capillary process. In the course of the detection, we observed that the content of Tween-20 in the loading buffer had correlation with the capillary displacement of MQBs on the NC membrane, which related to the FI after removing the background noise. Hence, four different contents of Tween-20 in loading buffer were employed to detect IAV virions at a moderate concentration (1×10^3 pfu mL^{-1}). The histogram in Fig. 3**D** showed that the loading buffer containing 2% Tween-20 had the maximum value of SNR. Thus, this concentration of Tween-20 was applied in the optimized condition to ameliorate the MQBs-based LFA.

3.4. Acquisition and analysis of fluorescence signal

In this device, the fluorescence signals were excited by ultraviolet LED light, recorded by the smartphone-based fluorescence reader, and further processed by the in-house built APP algorithm. The background signal, arising from two sources: the interference signal of ambient light and excitation light, and the fluorescence signal of MQBs induced by nonspecific adsorption and steric hindrance of the NC membrane, should be removed to improve the SNR value. Such that, the entire optical path was blocked by a well coupled 3D-printed enclosure, and an excitation optical filter and an emission filter were utilized to minimize the interference signal. Specifically, an in-house built APP algorithm can further denoise the obtained signal after the above-mentioned reduction of physical noise. Briefly, the red channel signal of the selected rectangle area (width = 500 pixels, height = 2600 pixels) covering the T and C lines was extracted (Fig. 4**A-B**). Subsequently, the raw fluorescence luminance distribution curve of the initial image was formed by adding up the red pixel values of each row along the black arrow and collecting the data of each row along the red arrow (Fig. 4**C-D**). Then, the baseline signals were removed to reduce the effect of nonspecific adsorption (Fig. 4**E-F**). The peak values at T and C lines were recognized as the processed fluorescence intensity.

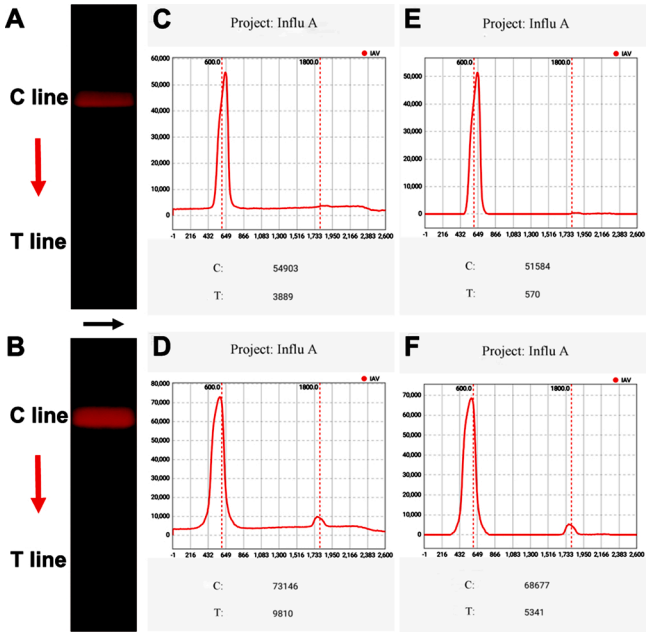

Fig. 4. Images of (A) negative and (B) positive test strip. The fluorescence intensity curves of (C) negative and (D) positive test strip, and (E-F) their corresponding noise-removed curves.

3.5. Analytical performance of MQBs-based LFA for IAV detection

Under the optimized conditions, we evaluated the performance of the MQBs-based LFA for quantification of IAV H1N1 virions with titers ranging from 10 to 1×10^6 pfu mL^{-1} in triplicate. As shown in Fig. 5A, the red-colored bands on the T line were brightened up with the increasing concentrations of IAV virions, and the signal for 500 pfu mL^{-1} of IAV virions can be clearly distinguished from the negative one by the naked eyes. Then, their corresponding signal values were read out by the analysis algorithm (Fig. 5B). The regression curve was fitted by $y = 89128.44 + (3514.68 - 89128.44)/(1 + (x/5381.76)^{1.16})$, $R^2 = 0.99984$, where x and y represent the IAV virion concentration and the FI value, respectively. The average of the negative results plus three times standard deviation was applied to estimate the limit of detection (LOD) as 22 pfu mL^{-1} of H1N1 virions in this assay. As a contrast, the LOD of commercial gold nanoparticles-based colorimetric LFA is ~2200 times higher as 5×10^4 pfu mL^{-1} (**Fig. S9**). To further verify the versatility of the MQBs-based LFA, the HAdV virions at different concentrations were also detected by using this system. As shown in **Fig. S10A**, the signal for 1000 pfu mL^{-1} can be clearly identified by naked eyes. Their corresponding signal values were read out and the LOD was estimated as 97 pfu mL^{-1} of HAdV virions (**Fig. S10B**). Compared with several other immunoassays, LFAs generally suffer from poor detection sensitivity despite the short assay time. In the proposed LFA, antibody-conjugated MQBs were able to directly enrich and fluorescently label IAV virions without an additional viral lysis step in the case for detection of influenza nucleoprotein target, thus greatly improving the sensitivity of LFA with simplified detection procedure and reduced assay time. Given that one plaque is usually formed by 100-1000 virions, the proposed MQBs-based fluorescent LFA can achieve an excellent overall analytical performance regarding the detection procedure, assay time, and detection sensitivity, as compared with some other immunoassays listed in **Table S1**.

The specificity of the MQBs-based LFA was estimated by detecting two subtypes of H1N1 and several other common respireviruses, namely, H1N1 FM1/A strain (1×10^5 pfu mL^{-1}), H1N1 2009/A strain (1×10^5 pfu mL^{-1}), HAdV5 (1×10^5 pfu mL^{-1}), HAdV55 (1×10^5 pfu mL^{-1}), and IBV (1×10^4 pfu mL^{-1}). As shown in Fig. 5C, the optimized MQBs-based LFA exhibited obvious signals for these two H1N1 strains, and obscure signals for the other respireviruses. As a consequence, the MQBs-based LFA has a good specificity for H1N1 virions and is insensitive to other respiratory viruses. As shown in **Fig. S11**, a good reproducibility was also verified by using 12 independent tests, of which the coefficient of variation was 9.21%.

3.6. Clinical sample tests

The clinical applicability of our magnetic-enrichment detection system was further confirmed by testing IAV virions spiked nasopharyngeal swabs, which were often used as the clinical specimen collection format. Nasopharyngeal swabs of 12 healthy people were collected and dissolved into 0.5 mL diluent as recommended in some commercial kits to ensure the universality of the detection. The H1N1 virions at different concentrations were then spiked into the diluent and tested by the presented optimized assay. The MQBs-based LFA was evaluated by its quantitative analysis ability and stability performance. As shown in Table 1, the average recoveries ranged from 90.1% to 108%, meanwhile this platform exhibited a relative low coefficient of variation (CV) ranging from 3.09% to 12.07%, indicating a good accuracy and stability for clinical sample detection via MQBs-based LFA.

4. Conclusions

In summary, we established a highly-sensitive MQBs-based LFA platform to detect IAV virions from clinical specimen. MQBs with a superparamagnetic $MnFe_2O_4$ magnetic core and numerous electrostatically-adsorbed red-colored QDs were prepared and further conjugated with IAV-specific antibody to serve as the enrichment substrate and fluorescent label in LFA. This system greatly improved the detection sensitivity and reduced the interference of complex biological

Table 1
Recovery results for H1N1 virions spiked in nasopharyngeal swab diluent.

Added concentration (pfu/mL)	Found concentration (pfu/mL)	Recovery (%)	CV (%)
2000	2040.70 ± 246.43	102.03	12.07
1000	980.27 ± 103.45	98.02	10.55
500	450.40 ± 13.92	90.08	3.09
100	108.05 ± 11.25	108.05	10.41

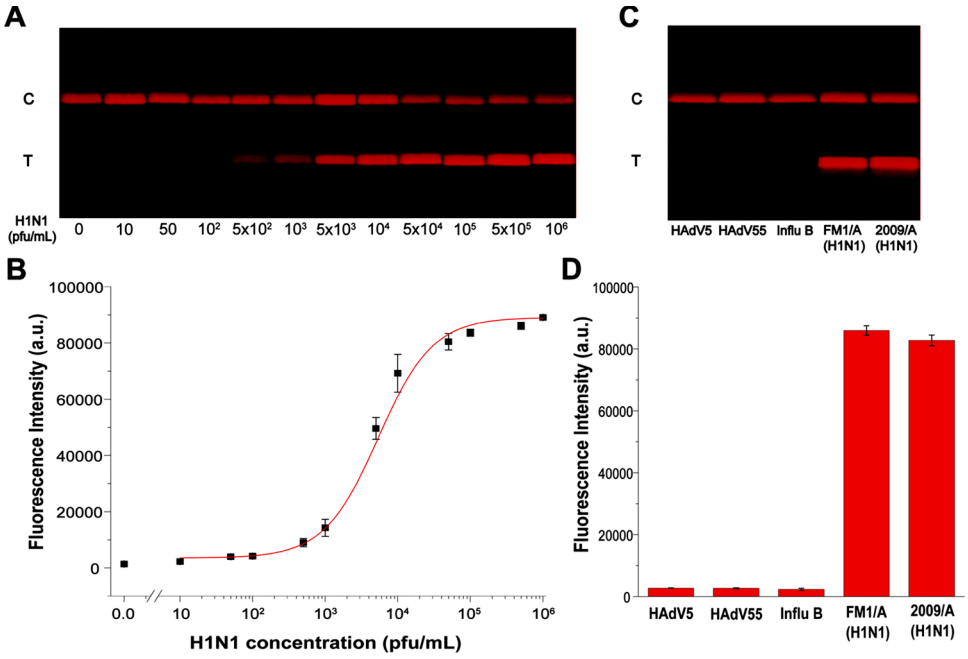

Fig. 5. MQBs-based fluorescent LFA for quantitative and specific detection of IAV H1N1 virions. (A) Images of the test strips at different concentrations of H1N1 virions in the range of 10–1×10^6 pfu mL^{-1}. (B) Corresponding fluorescence intensities on T line and the fitting curve. (C) Images and (D) corresponding fluorescence intensities of the test strips for HAdV5, HAdV55, Influ B, H1N1 FM1/A strain, and H1N1 2009/A strain. Error bars represent the standard deviation of three repetitive experiments.

matrix through multiple approaches, including magnetic separation and enrichment of target analytes, enhancement of fluorescence intensity, and elimination of background signal. This assay can achieve a low LOD of 22 pfu mL^{-1} of H1N1 virions in buffer within 35 min. A good specificity toward two H1N1 virus strains was verified by testing several other respiratory viruses, such as HAdV5, HAdV55, and IBV. The assay was also applied to detect IAV virions spiked in nasopharyngeal swab dilutions, and a superior clinical feasibility was indicated. Our further efforts will be focused on the detection of more IAV stains in clinical specimens. Given its excellent analytical performance, we believe that the presented MQBs-based LFA platform is a promising analytical approach for the direct detection of IAV virions in clinical biological samples.

CRediT authorship contribution statement

Zikun Bai: Methodology, Writing - original draft. **Hongjuan Wei:** Methodology, Writing - original draft. **Xingsheng Yang:** Methodology. **Yanhui Zhu:** Methodology. **Yongjin Peng:** Methodology. **Jing Yang:** Methodology. **Chongwen Wang:** Writing - review & editing, Supervision. **Zhen Rong:** Writing - review & editing, Supervision. **Shengqi Wang:** Writing - review & editing, Supervision.

Declaration of Competing Interest

The authors report no declarations of interest.

Acknowledgements

This study was supported by the National Natural Science Foundation of China (Grant no. 81902159), and the National S&T Major Project for Infectious Diseases Control (2018ZX10712001-010, 2018ZX10101003-001).

Appendix A. Supplementary data

Supplementary material related to this article can be found, in the online version, at doi:https://doi.org/10.1016/j.snb.2020.128780.

References

[1] J.K. Taubenberger, D.M. Morens, The pathology of influenza virus infections, Annu Rev Pathol 3 (2008) 499–522.
[2] J.S. Oxford, D. Gill, Unanswered questions about the 1918 influenza pandemic: origin, pathology, and the virus itself, The Lancet Infectious Diseases 18 (2018) e348-e54.
[3] V.C. Cheng, K.K. To, H. Tse, I.F. Hung, K.Y. Yuen, Two years after pandemic influenza A/2009/H1N1: what have we learned? Clin Microbiol Rev 25 (2012) 223–263.
[4] M.A. Rolfes, I.M. Foppa, S. Garg, B. Flannery, L. Brammer, J.A. Singleton, et al., Annual estimates of the burden of seasonal influenza in the United States: A tool for strengthening influenza surveillance and preparedness, Influenza and other respiratory viruses 12 (2018) 132–137.
[5] E. Williams, A. Dennison, A.W. Jenney, D.W. Spelman, Improvement in turnaround time for rapid respiratory virus testing using Xpert(R) Flu/RSV: a retrospective cohort study during a high incidence influenza season, Diagn Microbiol Infect Dis 95 (2019), 114869.
[6] K. Mitamura, H. Shimizu, M. Yamazaki, M. Ichikawa, T. Abe, Y. Yasumi, et al., Clinical evaluation of ID NOW influenza A & B 2, a rapid influenza virus detection kit using isothermal nucleic acid amplification technology - A comparison with currently available tests, J Infect Chemother (2019).
[7] Y.-D. Ma, Y.-S. Chen, G.-B. Lee, An integrated self-driven microfluidic device for rapid detection of the influenza A (H1N1) virus by reverse transcription loop-mediated isothermal amplification, Sensors and Actuators B: Chemical 296 (2019), 126647.
[8] R.W. Chan, M.C. Chan, J.M. Nicholls, J.S. Malik Peiris, Use of ex vivo and in vitro cultures of the human respiratory tract to study the tropism and host responses of highly pathogenic avian influenza A (H5N1) and other influenza viruses, Virus Res 178 (2013) 133–145.
[9] S. Carr, Seasonal and pandemic influenza: an overview with pediatric focus, Adv Pediatr 59 (2012) 75–93.
[10] J. Rahamat-Langendoen, H. Groenewoud, J. Kuijpers, W.J.G. Melchers, G.J. van der Wilt, Impact of molecular point-of-care testing on clinical management and in-hospital costs of patients suspected of influenza or RSV infection: a modeling study, J Med Virol 91 (2019) 1408–1414.
[11] W. Maneeprakorn, S. Bamrungsap, C. Apiwat, N. Wiriyachaiporn, Surface-enhanced Raman scattering based lateral flow immunochromatographic assay for sensitive influenza detection, RSC Advances 6 (2016) 112079–112085.
[12] T.T. Le, P. Chang, D.J. Benton, J.W. McCauley, M. Iqbal, A.E.G. Cass, Dual Recognition Element Lateral Flow Assay Toward Multiplex Strain Specific Influenza Virus Detection, Analytical chemistry 89 (2017) 6781–6786.
[13] Y.T. Tseng, C.H. Wang, C.P. Chang, G.B. Lee, Integrated microfluidic system for rapid detection of influenza H1N1 virus using a sandwich-based aptamer assay, Biosens Bioelectron 82 (2016) 105–111.
[14] R.Q. Zhang, S.L. Hong, C.Y. Wen, D.W. Pang, Z.L. Zhang, Rapid detection and subtyping of multiple influenza viruses on a microfluidic chip integrated with controllable micro-magnetic field, Biosens Bioelectron 100 (2018) 348–354.
[15] L.-Y. Hung, T.-B. Huang, Y.-C. Tsai, C.-S. Yeh, H.-Y. Lei, G.-B. Lee, A microfluidic immunomagnetic bead-based system for the rapid detection of influenza infections: from purified virus particles to clinical specimens, Biomedical Microdevices 15 (2013) 539–551.
[16] R.R.G. Soares, F. Neumann, C.R.F. Caneira, N. Madaboosi, S. Ciftci, I. Hernandez-Neuta, et al., Silica bead-based microfluidic device with integrated photodiodes for the rapid capture and detection of rolling circle amplification products in the femtomolar range, Biosens Bioelectron 128 (2019) 68–75.
[17] D.A. Green, K. StGeorge, Rapid Antigen Tests for Influenza: Rationale and Significance of the FDA Reclassification, Journal of Clinical Microbiology 56 (2018).
[18] K. Agoritsas, K. Mack, B.K. Bonsu, D. Goodman, D. Salamon, M.J. Marcon, Evaluation of the Quidel QuickVue test for detection of influenza A and B viruses in the pediatric emergency medicine setting by use of three specimen collection methods, J Clin Microbiol 44 (2006) 2638–2641.
[19] J. Yoon, S.G. Yun, J. Nam, S.H. Choi, C.S. Lim, The use of saliva specimens for detection of influenza A and B viruses by rapid influenza diagnostic tests, J Virol Methods 243 (2017) 15–19.
[20] J. Choi, M. Jeun, S.S. Yuk, S. Park, J. Choi, D. Lee, et al., Fully Packaged Portable Thin Film Biosensor for the Direct Detection of Highly Pathogenic Viruses from On-Site Samples, ACS nano (2018).
[21] F. Wu, H. Yuan, C. Zhou, M. Mao, Q. Liu, H. Shen, et al., Multiplexed detection of influenza A virus subtype H5 and H9 via quantum dot-based immunoassay, Biosensors & bioelectronics 77 (2016) 464–470.
[22] Z. Rong, Z. Bai, J. Li, H. Tang, T. Shen, Q. Wang, et al., Dual-color magnetic-quantum dot nanobeads as versatile fluorescent probes in test strip for simultaneous point-of-care detection of free and complexed prostate-specific antigen, Biosensors and Bioelectronics 145 (2019), 111719.
[23] L. Guo, Y. Shao, H. Duan, W. Ma, Y. Leng, X. Huang, et al., Magnetic Quantum Dot Nanobead-Based Fluorescent Immunochromatographic Assay for the Highly Sensitive Detection of Aflatoxin B1 in Dark Soy Sauce, Anal Chem 91 (2019) 4727–4734.
[24] J. Hu, Y.-Z. Jiang, M. Tang, L.-L. Wu, H.-y. Xie, Z.-L. Zhang, et al., Colorimetric-Fluorescent-Magnetic Nanosphere-Based Multimodal Assay Platform for Salmonella Detection, Anal Chem 91 (2019) 1178–1184.
[25] Z. Huang, J. Peng, J. Han, G. Zhang, Y. Huang, M. Duan, et al., A novel method based on fluorescent magnetic nanobeads for rapid detection of Escherichia coli O157:H7, Food chemistry 276 (2019) 333–341.
[26] J. Wang, X. Wu, C. Wang, Z. Rong, H. Ding, H. Li, et al., Facile Synthesis of Au-Coated Magnetic Nanoparticles and Their Application in Bacteria Detection via a SERS Method, ACS applied materials & interfaces 8 (2016) 19958–19967.
[27] J. Wang, X. Wu, C. Wang, Z. Rong, H. Ding, H. Li, et al., Facile Synthesis of Au-Coated Magnetic Nanoparticles and Their Application in Bacteria Detection via a SERS Method, ACS Appl Mater Interfaces 8 (2016) 19958–19967.
[28] X. Peng, G. Luo, Z. Wu, W. Wen, X. Zhang, S. Wang, Fluorescent-Magnetic-Catalytic Nanospheres for Dual-Modality Detection of H9N2 Avian Influenza Virus, ACS Appl Mater Interfaces 11 (2019) 41148–41156.
[29] Z. Wu, T. Zeng, W.J. Guo, Y.Y. Bai, D.W. Pang, Z.L. Zhang, Digital Single Virus Immunoassay for Ultrasensitive Multiplex Avian Influenza Virus Detection Based on Fluorescent Magnetic Multifunctional Nanospheres, ACS Appl Mater Interfaces 11 (2019) 5762–5770.

Zikun Bai is a master student in Beijing Institute of Radiation Medicine. His work focuses on the development of nanoparticle-based biosensors.

Hongjuan Wei is a master student in Beijing Institute of Radiation Medicine. Her work focuses on the development of nanoparticle-based biosensors.

Xingsheng Yang is a master student under the guidance of Dr. Chongwen Wang at Anhui agricultural University in China. His work focuses on the development of nanoparticle-based biosensors.

Yanhui Zhu is a Ph.D. student of Beijing Institute of Radiation Medicine. Her work focuses on virology.

Yongjin Peng is a master student in Beijing Institute of Radiation Medicine. His work focuses on the development of nanoparticle-based biosensors.

Jing Yang is currently a professor in Beijing Institute of Radiation Medicine. Her research interest focuses on the development of antiviral drugs and vaccines.

Chongwen Wang received his Ph.D. in biomedical engineering from Beijing University of Technology in 2018. He is currently an associate professor in Anhui Agricultural University. His work focuses on the preparation and application of novel metal and magnetic nanomaterials.

Zhen Rong received his bachelor degree in electrical engineering from Peking University in 2011, and Ph.D. in pharmaceutical analysis from Beijing Institute of Radiation Medicine in 2016. He is currently an assistant professor in Beijing Institute of Radiation Medicine. His research interest focuses on the development of nanophotonics biosensors and microfluidics devices.

Shengqi Wang is currently a professor in Beijing Institute of Radiation Medicine. His research interests include DNA/protein biosensing, virology, and pharmacology.